

Performance analysis of MPPM FSO transmission over Gamma–Chi-square strong atmospheric turbulence

JELENA TODOROVIC^{1,*}, PETAR SPALEVIC¹, STEFAN PANIC²,
MAJID HAMID ABDULLAH³, IVAN PANTELIC⁴

¹Faculty of Technical Sciences, University of Pristina in Kosovska Mitrovica,
Knjaza Milosa 7, 38220 Kosovska Mitrovica, Serbia

²Faculty of Sciences and Mathematics, University of Pristina in Kosovska Mitrovica,
Lole Ribara 29, 38220 Kosovska Mitrovica, Serbia

³School of Informatics and Computing, Singidunum University,
Danijelova 32, 11000 Belgrade, Serbia

⁴Valjevo Business School of Applied Studies, Western Serbia Academy of Applied Studies,
Trg Svetog Save 34, 31000 Uzice, Serbia

*Corresponding author: jelena.todorovic@pr.ac.rs

In this paper, performance analysis of free space optical (FSO) system operating in conditions of strong atmospheric turbulence over Gamma–Chi-square turbulence model, has been carried out. We have observed reception over multi-pulse pulse-position (MPPM) modulation format for the case of strong atmospheric turbulence conditions modeled with Gamma–Chi-square turbulence model and have compared it with turbulence modeling distributions such are: Gamma–Gamma distribution, K -distribution, negative exponential distribution, log–normal distribution. First, we have provided closed-form analytical expressions for average bit error rate (ABER) at the reception for each observed case and then based on them, we have obtained numerical and Monte Carlo simulation results in order to observe turbulence level impact on system performance.

Keywords: FSO – free space optical, ABER – average bit error rate, MPPM – multi-pulse pulse-position, novel Gamma–Chi-square distribution, channel model, strong atmospheric turbulence.

1. Introduction

The free space optics (FSO) represents promising technology for short-range wireless communications, access to the last mile and laser communication in free space. The FSO technology is easily available and capable of providing a low bit error rate, as well as high data transmission speed to several kilometers and high optical bandwidth [1–4].

Despite the main advantages of the FSO technology, widespread use has been disrupted by the connection reliability, especially on large distances, due to fading caused by atmospheric turbulence and weather condition sensitivity [1,5–8]. Strong atmospheric turbulence is one of the major challenges in the implementation of signal transmission via the FSO system. The negative impacts of atmospheric turbulence include scintillations, distortions, phase change, beam spreading and displacement of the beam in the vertical and horizontal directions. This results in significant deterioration of system performance, especially in long distance transmission of several kilometers, when the signal will come across a strong turbulence [9–11].

Different techniques are applied to improve the performance of the FSO links in different weather and turbulence conditions. A large number of different channel distribution models for modeling different levels of atmospheric turbulence have been proposed: Gamma–Gamma [12], log–normal [13], negative exponential [14], K -distribution [15], I – K distribution [16], Rician distribution [17], Weibull distribution [15], exponential Weibull distribution [18], double-generalized Gamma distribution [15], Málaga distribution [6] and others.

The proposed models are often investigated for different modulation formats applicable to the FSO system to get the most reliable signal transmission. In [9,19–21] the FSO systems performance in different conditions for different modulation schemes are analyzed, for BPSK-SIM, DPSK, DPSK-SIM, OOK, QPSK, PPM, MPPM, MPSK, M-QAM, PolSK modulation. OOK modulation format is most commonly used due to simple implementation and high bandwidth efficiency. However, in some cases, and especially when it comes to the power limitation, it is better to use modulating schemes such as PPM. Compared to other modulation techniques, PPM offers the highest power efficiency, with the increase in bandwidth and the system complexity [18]. BER performance has been improved because PPM symbols are orthogonal, so the pulses are not overlapping [22]. Each pulse of laser can be used to represent one or more bits of information by its position in time relative to start of a symbol whose duration is identical to that of information bits it contains [9]. As an alternative to standard PPM and OOK modulation scheme, MPPM modulation was proposed. This modulation technique is a compromise between PPM and OOK, because it offers better bandwidth efficiency compared to PPM and better power efficiency compared to OOK technique [23,24].

Motivated by the possibilities provided by the MPPM modulation technique, in this paper we have analyzed the performance of a system modulated by MPPM modulation and operating in conditions of strong atmospheric turbulence. A performance comparison is given for some existing channel distribution models and for the novel Gamma–Chi-square distribution, whose closed-form PDF expressions were obtained and presented in [25]. In [25] it is shown that Gamma–Chi-square distribution can efficiently model turbulence eddy effects in a wide range of conditions.

The manuscript is organized as follows. In Section 2, the analyzed system model is given, *i.e.*, all considered channel distribution models are presented. In Section 3, the initial expressions for the ABER calculation are given and analytical closed-form expressions for ABER are derived and presented for all considered distributions. The ob-

tained numerical results are presented and discussed in Section 4, for different signal strength, link distance, turbulence level and time slots. Section 5 summarizes the conclusions.

2. System model

The PDF for the Gamma–Gamma model is given by the expression [12]:

$$f(I) = \frac{2(\alpha\beta)^{\frac{\alpha+\beta}{2}}}{\Gamma(\alpha)\Gamma(\beta)} I^{\frac{\alpha+\beta}{2}-1} K_{\alpha-\beta}(2\sqrt{\alpha\beta I}) \quad (1)$$

where I is irradiance at the receiver, $\Gamma(\cdot)$ represents the Gamma function [26, Eq. 8.310], and $K_v(\cdot)$ v -th-order modified Bessel function of the second kind [26, Eq. 8.432]. The parameters α and β are the effective numbers of small-scale and large-scale eddies of the scattering environment, respectively. These are parameters of the atmospheric turbulence that for propagation of plane waves and zero inner scale can be expressed as [12]

$$\alpha = \left\{ \exp \left[\frac{0.49\sigma_R^2}{(1 + 0.11\sigma_R^{12/5})^{7/6}} \right] - 1 \right\}^{-1} \quad (2)$$

$$\beta = \left\{ \exp \left[\frac{0.51\sigma_R^2}{(1 + 0.69\sigma_R^{12/5})^{5/6}} \right] - 1 \right\}^{-1} \quad (3)$$

where σ_R^2 represents the Rytov variance used to determine the intensity of the optical signal due to atmospheric turbulence. It is defined as

$$\sigma_R^2 = 1.23 C_n^2 k^{7/6} L^{11/6} \quad (4)$$

where $k = 2\pi/\lambda$ is an optical wave number with wavelength λ , while L is the distance between the transmitter and the receiver, *i.e.*, the length of the optical signal propagation. The parameter C_n^2 represents the index of refraction used as a measure of the turbulence strength, which typically ranges from 10^{-17} to $10^{-13} \text{ m}^{-2/3}$ for channels from weak to strong turbulence, respectively.

The K -distribution represents a product of the exponential and Gamma distributions. The K -distribution of the irradiance at the receiver is given by [15]

$$f_I(I) = \frac{2\alpha^{\frac{\alpha+1}{2}}}{\Gamma(\alpha)} I^{\frac{\alpha-1}{2}} K_{\alpha-1}(2\sqrt{\alpha I}) \quad (5)$$

where the parameter α is defined by Eq. (2).

The PDF for the negative exponential model is given by the expression [14, 15]

$$f_I(I) = \frac{1}{I_0} \exp\left(-\frac{I}{I_0}\right) \quad (6)$$

where I_0 is the mean irradiance.

The log-normal distribution of the irradiance at the receiver is given by [13]

$$f_I(I) = \frac{1}{\sqrt{2\pi\sigma^2}} \frac{1}{I} \exp\left\{-\frac{1}{2\sigma^2} \left[\ln(I) + \frac{\sigma^2}{2}\right]^2\right\} \quad (7)$$

The parameter σ is the scintillation index defined by Eq. (4) [13].

The novel Gamma–Chi-square irradiance PDF model is given by [25]

$$\begin{aligned} f_{I_a}(I_a) &= \sum_{m=0}^{\infty} \frac{2K^m e^{-K}}{\Gamma(\alpha)\Gamma(m+1)m!} \left(\frac{\alpha(1+K)}{\Omega_p}\right)^{\frac{\alpha+m+1}{2}} I_a^{\frac{\alpha+m-1}{2}} K_{\alpha-m-1} \left(2\sqrt{\frac{\alpha(1+K)}{\Omega_p} I_a}\right) \end{aligned} \quad (8)$$

where K is the ratio of the power of the LOS component to the average power of the scattered component [27], Ω_p is total received signal power and parameter α is defined by Eq. (2).

3. Average BER

For an optical MPPM modulated signal transmitted by FSO system, the probability of conditional BER over the received irradiance fluctuation can be represented as [23]

$$P_{ec}(I) = \frac{2^{\left[\log_2\binom{N}{\omega}\right]-1}}{2^{\left[\log_2\binom{N}{\omega}\right]}-1} \frac{\binom{N}{\omega}-1}{2} \operatorname{erfc}\left(\frac{Rp\left(\frac{\eta A}{\lambda L}\right)^2 I}{2\omega} \sqrt{\frac{N}{\sigma_N^2} \log_2\binom{N}{\omega}}\right) \quad (9)$$

where R is photodetector responsivity, p is the average transmitted optical power, η is the quantum efficiency of the detector, A is the detector area in m^2 , λ is the operating wavelength, L is the distance between transmitter and receiver and σ_N is noise standard deviation. Parameters N and ω represent time slots. In MPPM modulation techniques, signal frame period T is divided into N equal slots of duration $T_s = T/N$. In each frame period, only $1 \leq \omega \leq N$ slots would be active, *i.e.*, optical power is transmitted in ω time slots only [23, 28].

Average BER can be obtained by averaging Eq. (9) over the PDF of the irradiance at the receiver I , according to [29]

$$P_e = \int_0^\infty P_{ec}(I)f_I(I)dI \quad (10)$$

3.1. Gamma–Gamma distribution

In order to derive a closed-form expression for the ABER, the modified Bessel function of the second kind $K_v(\cdot)$ in Eq. (1) is represented by the Meijer G function as [26, Eq. 9.34.3]:

$$K_v(x) = \frac{1}{2} G_{0, 2}^{2, 0} \left[\frac{x^2}{4} \right]_{(v-2), -(v-2)} \quad (11)$$

and the complementary error function $\text{erfc}(\cdot)$ in Eq. (9) is represented by the Meijer G function as [30, Eq. 06.27.26.0003.01]

$$\text{erfc}(x) = 1 - \frac{x}{\sqrt{\pi}} G_{1, 2}^{1, 1} \left[x^2 \right]_{0, -1/2}^{1/2} \quad (12)$$

By substituting Eq. (1) and Eq. (9) into Eq. (10), and making use of the relationships given in Eq. (11) and Eq. (12), as well as by using the solutions of the resulting integral given by [26, Eq. 7.811.4] and [31, Eq. 07.34.21.0012.01], we derive the ABER closed-form expression as follows:

$$P_e = \frac{2^{\left[\log_2\left(\frac{N}{\omega}\right)\right]-1}}{2^{\left[\log_2\left(\frac{N}{\omega}\right)\right]-1}} \frac{\left(\frac{N}{\omega}\right)-1}{2} \left\{ 1 - \frac{1}{\alpha\beta\Gamma(\alpha)\Gamma(\beta)} \frac{Rp\left(\frac{\eta A}{\lambda L}\right)^2}{2\sqrt{\pi}\omega} \sqrt{\frac{N}{\sigma_N^2} \log_2\left(\frac{N}{\omega}\right)} \right. \\ \times H_{3, 2}^{1, 3} \left[\left(\frac{Rp}{2\alpha\beta\omega} \right)^2 \left(\frac{\eta A}{\lambda L} \right)^4 \frac{N}{\sigma_N^2} \log_2\left(\frac{N}{\omega}\right) \right]_{(0, 1), \left(-\frac{1}{2}, 1\right)}^{\left(\frac{1}{2}, 1\right), (-\alpha, 2), (-\beta, 2)} \left. \right\} \quad (13)$$

3.2. K-distribution

By substituting Eq. (5) and Eq. (9) into Eq. (10), by making use of the relationships given in Eq. (11) and Eq. (12), as well as by using the solutions of the resulting integral

given by [26, Eq. 7.811.4] and [31, Eq. 07.34.21.0012.01], we derive the ABER expression as follows:

$$P_e = \frac{2^{\left[\log_2\left(\frac{N}{\omega}\right)\right]-1}}{2^{\left[\log_2\left(\frac{N}{\omega}\right)\right]-1}} \frac{\left(\frac{N}{\omega}\right)-1}{2} \left\{ 1 - \frac{1}{\alpha \Gamma(\alpha)} \frac{Rp \left(\frac{\eta A}{\lambda L}\right)^2}{2\sqrt{\pi} \omega} \sqrt{\frac{N}{\sigma_N^2} \log_2\left(\frac{N}{\omega}\right)} \right. \\ \left. \times H_{3,2}^{1,3} \left[\left(\frac{Rp}{2\alpha\omega} \right)^2 \left(\frac{\eta A}{\lambda L} \right)^4 \frac{N}{\sigma_N^2} \log_2\left(\frac{N}{\omega}\right) \middle| \begin{array}{l} \left(\frac{1}{2}, 1\right), (-\alpha, 2), (-1, 2) \\ (0, 1), \left(-\frac{1}{2}, 1\right) \end{array} \right] \right\} \quad (14)$$

3.3. Negative exponential distribution

By substituting Eq. (6) and Eq. (9) into Eq. (10), using the relationship given in Eq. (12) and the identity [32, Eq. 8.4.3],

$$e^{-x} = G_{0,1}^{1,0} \left[x \Big|_0^- \right] \quad (15)$$

as well as using the solutions of the resulting integral given by [24, Eq. 3.310] and [31, Eq. 07.34.21.0012.01], we derive the ABER expression as follows:

$$P_e = \frac{2^{\left[\log_2\left(\frac{N}{\omega}\right)\right]-1}}{2^{\left[\log_2\left(\frac{N}{\omega}\right)\right]-1}} \frac{\left(\frac{N}{\omega}\right)-1}{2} \left\{ 1 - \frac{Rp \left(\frac{\eta A}{\lambda L}\right)^2 I_0}{2\sqrt{\pi} \omega} \sqrt{\frac{N}{\sigma_N^2} \log_2\left(\frac{N}{\omega}\right)} \right. \\ \left. \times H_{2,2}^{1,2} \left[\left(\frac{Rp I_0}{2\omega} \right)^2 \left(\frac{\eta A}{\lambda L} \right)^4 \frac{N}{\sigma_N^2} \log_2\left(\frac{N}{\omega}\right) \middle| \begin{array}{l} \left(\frac{1}{2}, 1\right), (-1, 2) \\ (0, 1), \left(-\frac{1}{2}, 1\right) \end{array} \right] \right\} \quad (16)$$

3.4. Log-normal distribution

By substituting Eq. (7) and Eq. (9) into Eq. (10), by making use of the variable change $t = [\ln I + \sigma^2/2]/\sqrt{2}\sigma$ and identity [30, Eq. 06.27.02.0001.01],

$$\text{erfc}(x) = 1 - \frac{2}{\sqrt{\pi}} \sum_{n=0}^{\infty} \frac{(-1)^n x^{2n+1}}{n! (2n+1)} \quad (17)$$

as well as by using the solutions of the resulting integral given by [33, Eq. 01.03.21. 0029.01] and [26, Eq. 3.322.2], we derive the ABER expression as follows:

$$\begin{aligned}
 P_e = & \frac{2^{\left[\log_2\binom{N}{\omega}\right]-1}}{2^{\left[\log_2\binom{N}{\omega}\right]-1}} \frac{\binom{N}{\omega}-1}{2} \left\{ \frac{1}{2} - \sum_{n=0}^{\infty} \frac{(-1)^n}{n!(2n+1)} \right. \\
 & \times \left[\frac{Rp\left(\frac{\eta A}{\lambda L}\right)^2}{2\omega} \sqrt{\frac{N}{\sigma_N^2} \log_2\binom{N}{\omega}} \right]^{2n+1} \exp\left[\sigma^2 n(2n+1)\right] \\
 & \times \left. \left[1 - \operatorname{erf}\left(-\frac{\sqrt{2}}{2} \sigma(2n+1)\right) \right] \right\} \quad (18)
 \end{aligned}$$

3.5. Gamma–Chi-square distribution

In order to derive the ABER closed-form expression for atmospheric turbulence Gamma–Chi-square channel model, the similar procedure applies as in the previous cases for other distributions.

By substituting Eq. (8) and Eq. (9) into Eq. (10), by making use of the relationships given in Eq. (11) and Eq. (12), as well as by using the solutions of the resulting integral given by [26, Eq. 7.811.4] and [31, Eq. 07.34.21.0012.01], we derive the ABER expression as follows:

$$\begin{aligned}
 P_e = & \sum_{m=0}^{\infty} \frac{2^{\left[\log_2\binom{N}{\omega}\right]-1}}{2^{\left[\log_2\binom{N}{\omega}\right]-1}} \frac{\binom{N}{\omega}-1}{2} \frac{K^m e^{-K}}{m!} \left\{ 1 - \frac{\Omega_p}{\alpha(1+K)\Gamma(\alpha)\Gamma(m+1)} \right. \\
 & \times \frac{Rp\left(\frac{\eta A}{\lambda L}\right)^2}{2\sqrt{\pi}\omega} \sqrt{\frac{N}{\sigma_N^2} \log_2\binom{N}{\omega}} \\
 & \times H_{3,2}^{1,3} \left[\left(\frac{Rp\Omega_p}{2\omega\alpha(1+K)} \right)^2 \left(\frac{\eta A}{\lambda L} \right)^4 \frac{N}{\sigma_N^2} \log_2\binom{N}{\omega} \right]_{\left(0,1\right),\left(-\frac{1}{2},1\right)}^{\left(\frac{1}{2},1\right),\left(-\alpha,2\right),\left(-m-1,2\right)} \left. \right\} \quad (19)
 \end{aligned}$$

4. Numerical results

In this section, the ABER performances of MPPM based FSO system are investigated. The FSO system for atmospheric channels modeled with Gamma–Gamma distribution, *K*-distribution, negative exponential distribution, and log–normal distribution is considered for different values of strong turbulence with indexes of reflection $C_n^2 = 1.2 \times 10^{-13} \text{ m}^{-2/3}$ and $C_n^2 = 2.5 \times 10^{-13} \text{ m}^{-2/3}$. In terms of the distance between transmitter and receiver, three cases were observed: $L = 0.5 \text{ km}$, $L = 1 \text{ km}$ and $L = 1.5 \text{ km}$. In addition, the impact of the number of active time slots ω on the ABER performance of FSO system with channels in strong turbulence is analyzed. Certain numerical results based on the analytical expressions for ABER derived in Sections 3, as a function of the average received optical power and atmospheric turbulence strength are graphically presented.

Some important FSO system parameters and their values considered in the numerical evaluations are presented in the Table.

Table. System parameter used for computation.

Parameter	Symbol	Value
Operating wavelength	λ	875 nm
Photodetector responsivity	R	0.5 A/W
Radius of circular detector aperture	a	0.05 m
Quantum efficiency	η	0.8
Noise standard deviation	σ_N	10^{-7} A/Hz
Average transmitted optical power	p	10^{-5} W
Time slots	N	12
Active time slots	ω	5

The ABER behavior for the FSO channel modeled with the Gamma–Gamma distribution as a function of the average received optical power is shown in Fig. 1. From Fig. 1, it can be seen that ABER decreases almost linearly with power increase. For higher values of strong atmospheric turbulence, as well as for longer distances between transmitter and receiver, ABER has higher values. Also, it can be observed that at the same link distance of $L = 0.5 \text{ m}$, ABER is higher by several orders of magnitude only because of the very small increase in atmospheric turbulence. A similar conclusion can be drawn if the change in link distance is observed over the same value of turbulence.

From Fig. 2 it can be seen that in the case of the atmospheric channel modeled with the *K*-distribution, small changes in the strong turbulence do not affect ABER too much. However, the length of the FSO link has a much greater impact on ABER here. ABER has higher values for the longer distance between the transmitter and the receiver. Still, this ABER increase in the *K*-distribution is not as significant high as in the atmospheric channel modeled with the Gamma–Gamma distribution. Although it

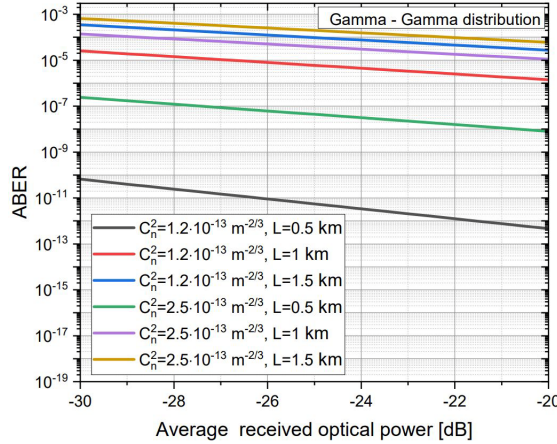


Fig. 1. ABER for the Gamma–Gamma distribution *versus* average received optical power for different values of the strong turbulence and link distance.

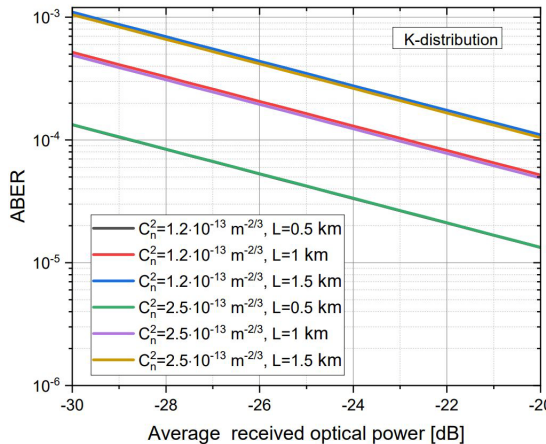


Fig. 2. ABER for the *K*-distribution *versus* average received optical power for different values of the strong turbulence and link distance.

can be observed that better ABER performance of FSO system is achieved with Gamma–Gamma distribution.

In Fig. 3, ABER changes are shown depending on the average received optical power in the FSO channel modeled with the Negative Exponential distribution. It is clearly depicted that the ABER for all the considered distribution shows an improvement with increasing power. As expected, for longer link distances the higher ABER values are obtained. Further, the FSO system performance is better for higher values of the mean irradiance I_0 , *i.e.*, it gives lower ABER values.

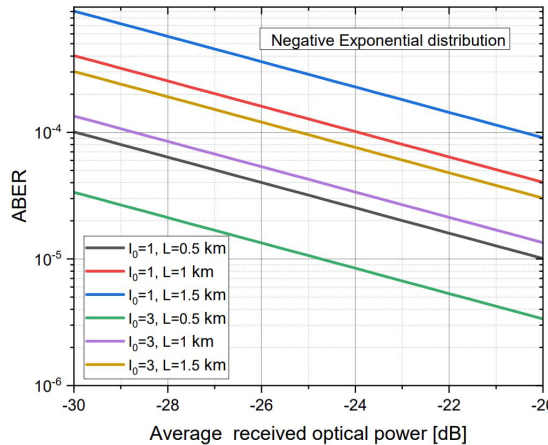


Fig. 3. ABER for the negative exponential distribution *versus* average received optical power for different values of the mean irradiance and link distance.

The ABER for FSO channel modeled with the log–normal distribution as a function of the average optical power obtained, shown in Fig. 4, gives the best results for shorter distances between the transmitter and the receiver. In this case, ABER has significantly lower values compared to the results obtained for other distributions by $L = 0.5 \text{ m}$, which leads to a significant improvement of this FSO system. On the other side, for longer link distances, the FSO system modeled with the log–normal distribution has very high ABER values, even several orders of magnitude higher than the Gamma–Gamma distribution and K -distribution for the same parameter values. From Fig. 4 it can be seen that even for small increases of strong turbulence and link distance ABER increases,

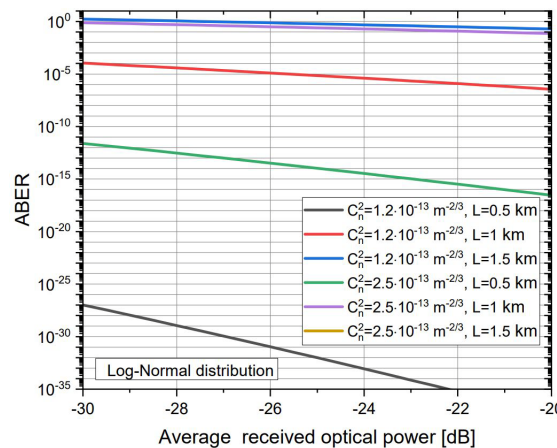


Fig. 4. ABER for the log–normal distribution *versus* average received optical power for different values of the strong turbulence and link distance.

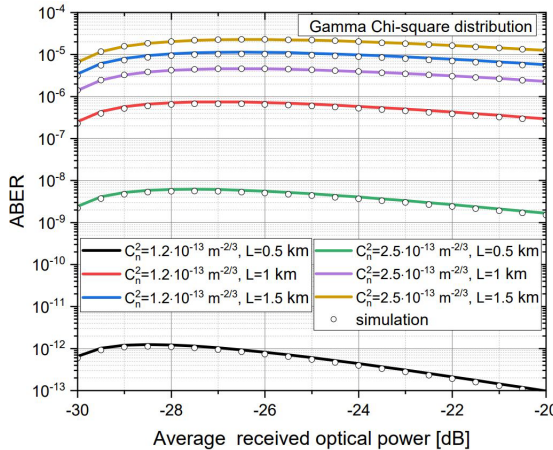


Fig. 5. ABER for the Gamma–Chi-square distribution *versus* average received optical power for different values of the strong turbulence and link distance.

i.e., it takes significantly higher values. For higher values of strong turbulence and longer link distances, ABER is almost constant with increasing power.

In the case of the novel Gamma–Chi-square distribution, from Fig. 5 it can be seen that with the increase in received optical power ABER is almost constant for longer link distances. At shorter distances, a decrease in ABER can be observed when power takes higher values. The difference in ABER values for different levels of atmospheric turbulence is more pronounced at shorter distances. FSO system with Gamma–Chi-square distribution gives better results in this case than Gamma–Gamma distribution, *i.e.*, ABER is lower in the same observed conditions. Also, the results are significantly better than with the K -distribution and the negative exponential distribution, while compared to the log–normal distribution Gamma–Chi-square distribution has a lower ABER only in the case of stronger atmospheric turbulence and longer link distances.

In Figs. 6–9, the ABER behavior is shown for the Gamma–Gamma distribution, K -distribution, log–normal distribution and Gamma–Chi-square distribution, respectively, for different values of the link distance and active time slots. From the given figures, it can be seen that an increase in the atmospheric turbulence strength principally leads to an increase in the ABER, with an exception that this increase has different effects in different distribution models.

In the case of the Gamma–Gamma distribution, it can be seen from Fig. 6 that for longer link distance ABER has higher values, but is almost constant with increasing atmospheric turbulence. For shorter link distances, ABER increases with increasing atmospheric turbulence. It can be observed that for received optical power $p = 10^{-5} \text{ W}$, using fewer active time slots improves the FSO system performance.

From Fig. 7, for the K -distribution it can be seen that link distance and active time slots have more impact on ABER than atmospheric turbulence. ABER is constant

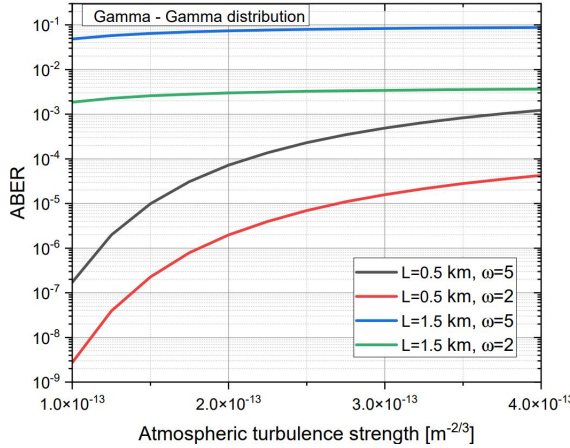


Fig. 6. ABER for the Gamma-Gamma distribution *versus* atmospheric turbulence strength for different values of the link distance and active time slots.

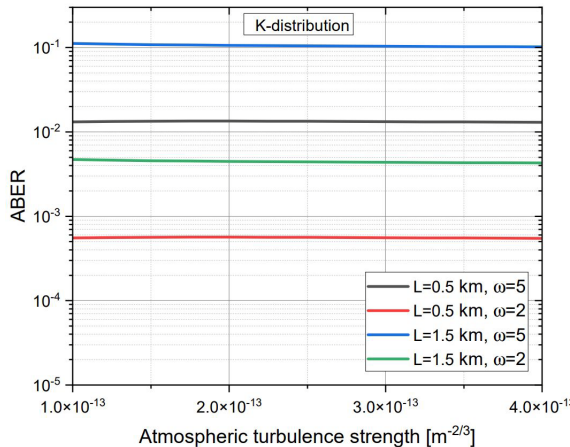


Fig. 7. ABER for the K -distribution *versus* atmospheric turbulence strength for different values of the link distance and active time slots.

throughout the range of changes in atmospheric turbulence values. The impact of active time slots is most reflected in the fact that for fewer active time slots, ABER has lower values, even if the link distance is increased.

For FSO system with the log-normal distribution, Fig. 8, for lower values of atmospheric turbulence, there is a large increase in ABER for longer link distances. For shorter link distances, ABER increases significantly with increasing atmospheric turbulence. The number of active time slots has a lot of impact here too, so once again it can be seen that for the given parameters the FSO system has better performance for fewer active time slots.

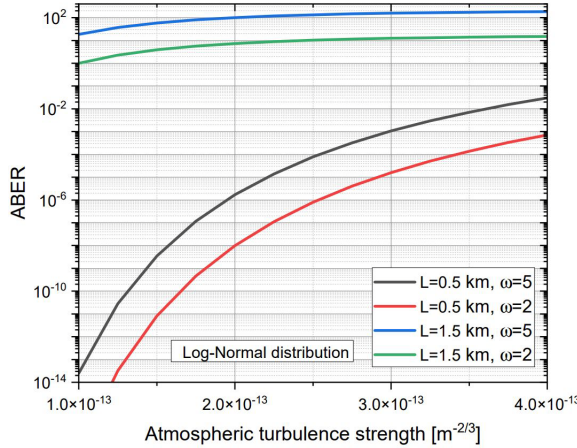


Fig. 8. ABER for the log–normal distribution *versus* atmospheric turbulence strength for different values of the link distance and active time slots.

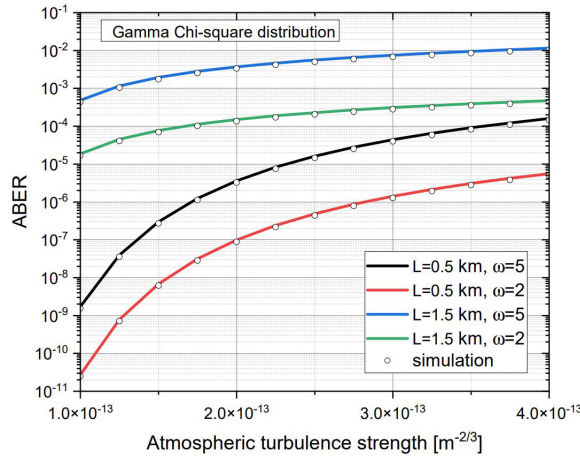


Fig. 9. ABER for the Gamma–Chi-square distribution *versus* atmospheric turbulence strength for different values of the link distance and active time slots.

As in previous cases, for the Gamma–Chi-square distribution ABER behaves similarly to changes in atmospheric turbulence, link distance and active time slots (Fig. 9). It can be seen that the FSO system has better performance in this case if Gamma–Chi-square distribution is applied, compared to Gamma–Gamma and K -distribution. At longer distances Gamma–Chi-square distribution gives better ABER results than log–normal distribution, while at shorter distances and weaker atmospheric turbulence it is best to use log–normal distribution for both smaller and larger number of active time slots. A continuous and smooth change of ABER can be seen with the change of the atmospheric turbulence in the Gamma–Chi-square model, while in the cases of

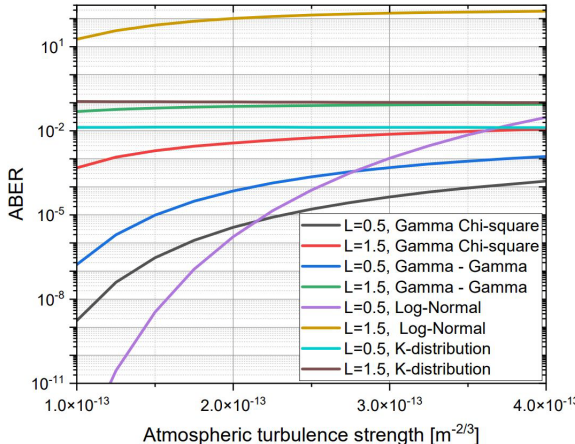


Fig. 10. ABER for different distribution *versus* atmospheric turbulence strength and for different values of the link distance.

other models these changes are not so gradual, so this distribution is most suitable for modeling ABER at reception.

From Figs. 5 and 9 it can be seen that the simulation results are approximately the same as the numerical results thus confirming the numerical results for novel Gamma–Chi-square distribution.

In Fig. 10 the ABER behavior is shown for different distributions and different values of the link distance and for active time slots $\omega = 5$.

5. Conclusion

In this paper, the signal reception in the FSO system whose channel is modeled with the Gamma–Gamma distribution, K -distribution, negative exponential distribution, log–normal distribution and Gamma–Chi-square distribution is observed. The obtained ABER values for the signals modulated by the MPPM modulation scheme both in function of average received optical power and in function of atmospheric turbulence strength are presented and analyzed. The FSO system has better performance, *i.e.*, ABER is lower for the same fit conditions, in case the channel is modeled with log–normal distribution for shorter distances, while when longer distances are analyzed, a novel Gamma–Chi-square distribution gives better results. Thus, we have provided lower and higher bound approximation for FSO transmission in strong turbulence conditions.

Based on the obtained results, the behavior of different implementations of channel distributions in FSO system can be predicted for different values of network parameters and in different propagation environments. Significant improvements open the way for future research in this area and use this paper as reference. This enables the designers of wireless optical systems to create rational systematic solutions for the desired system performance.

References

- [1] HENNIGER H., WILFERT O., *An introduction to free-space optical communications*, Radioengineering **19**(2), 2010: 203–212.
- [2] STEFANOVIC C., MORALES-CÉSPEDES M., ARMADA A.G., *Performance analysis of RIS-assisted FSO communications over Fisher-Snedecor F turbulence channels*, Applied Sciences **11**(21), 2021: 10149, DOI: [10.3390/app112110149](https://doi.org/10.3390/app112110149).
- [3] BADARNEH O.S., DERBAS R., ALMEHMADI F.S., EL BOUANANI F., MUHAIDAT S., *Performance analysis of FSO communications over F turbulence channels with pointing errors*, IEEE Communications Letters **25**(3), 2021: 926–930, DOI: [10.1109/lcomm.2020.3042489](https://doi.org/10.1109/lcomm.2020.3042489).
- [4] BABIC R., *Signal Analysis*, Akadembska Misao, Belgrade, Serbia, 2000.
- [5] HASAN O., TAHÀ M., *Optimized FSO system performance over atmospheric turbulence channels with pointing error and weather conditions*, Radioengineering **25**(4), 2016: 658–665, DOI: [10.13164/re.2016.0658](https://doi.org/10.13164/re.2016.0658).
- [6] BALAJI K.A., PRABU K., *BER analysis of relay assisted PSK with OFDM ROFSO system over Malaga distribution including pointing errors under various weather conditions*, Optics Communications **426**, 2018: 187–193, DOI: [10.1016/j.optcom.2018.05.027](https://doi.org/10.1016/j.optcom.2018.05.027).
- [7] FADHIL H.A., AMPHAWAN A., SHAMSUDDIN H.A. B., ABD T.H., AL-KHAFAJI H.M. R., ALJUNID S.A., AHMED N., *Optimization of free space optics parameters: An optimum solution for bad weather conditions*, Optik **124**(19), 2013: 3969–3973, DOI: [10.1016/j.ijleo.2012.11.059](https://doi.org/10.1016/j.ijleo.2012.11.059).
- [8] NDJONGUE A.R., NGATCHED T., DOBRE O., ARMADA A.G., HAAS H., *Analysis of RIS-based terrestrial-FSO link over G-G turbulence with distance and jitter ratios*, Journal of Lightwave Technology **39**(21), 2021: 6746–6758, DOI: [10.1109/JLT.2021.3108532](https://doi.org/10.1109/JLT.2021.3108532).
- [9] MALIK S., SAHU P.K., *Performance analysis of free space optical communication system using different modulation schemes over weak to strong atmospheric turbulence channels*, [In] *Optical and Wireless Technologies*, V. Janyani, G. Singh, M. Tiwari, A. d’Alessandro [Eds.], Lecture Notes in Electrical Engineering, Vol. 546, Springer, Singapore, 2019: 387–399, DOI: [10.1007/978-981-13-6159-3_41](https://doi.org/10.1007/978-981-13-6159-3_41).
- [10] PEPPAS K.P., MATHIOPoulos P.T., *Free space optical communication with spatial modulation and coherent detection over H-K atmospheric turbulence channels*, Journal of Lightwave Technology **33**(20), 2015: 4221–4232, DOI: [10.1109/JLT.2015.2465385](https://doi.org/10.1109/JLT.2015.2465385).
- [11] ARYA S., CHUNG Y.H., *Spectrum sensing for free space optical communications in strong atmospheric turbulence channel*, Optics Communications **445**, 2019: 24–28, DOI: [10.1016/j.optcom.2019.04.009](https://doi.org/10.1016/j.optcom.2019.04.009).
- [12] SANDALIDIS H.G., TSIFTSIS T.A., KARAGIANNIDIS G.K., *Optical wireless communications with heterodyne detection over turbulence channels with pointing errors*, Journal of Lightwave Technology **27**(20), 2009: 4440–4445, DOI: [10.1109/jlt.2009.2024169](https://doi.org/10.1109/jlt.2009.2024169).
- [13] YANG L., SONG X., CHENG J., HOLZMAN J.F., *Free-space optical communications over lognormal fading channels using OOK with finite extinction ratios*, IEEE Access **4**, 2016: 574–584, DOI: [10.1109/access.2016.2520936](https://doi.org/10.1109/access.2016.2520936).
- [14] NISTAZAKIS H.E., ASSIMAKOPOULOS V.D., TOMBRAS G.S., *Performance estimation of free space optical links over negative exponential atmospheric turbulence channels*, Optik **122**(24), 2011: 2191–2194, DOI: [10.1016/j.ijleo.2011.01.013](https://doi.org/10.1016/j.ijleo.2011.01.013).
- [15] ANBARASI K., HEMANTH C., SANGETHA R.G., *A review on channel models in free space optical communication systems*, Optics & Laser Technology **97**, 2017: 161–171, DOI: [10.1016/j.optlastec.2017.06.018](https://doi.org/10.1016/j.optlastec.2017.06.018).
- [16] PEPPAS K.P., STASSINAKIS A.N., TOPALIS G.K., NISTAZAKIS H.E., TOMBRAS G.S., *Average capacity of optical wireless communication systems over I-K atmospheric turbulence channels*, Journal of Optical Communications and Networking **4**(12), 2012: 1026–1032, DOI: [10.1364/jocn.4.001026](https://doi.org/10.1364/jocn.4.001026).
- [17] ZHOU H., XIE W., ZHANG L., BAI Y., WEI W., DONG Y., *Performance analysis of FSO coherent BPSK systems over Rician turbulence channel with pointing errors*, Optics Express **27**(19), 2019: 27062–27075, DOI: [10.1364/oe.27.027062](https://doi.org/10.1364/oe.27.027062).

- [18] AHMED M.M., AHMED K.T., HOSSAN A., HOSSAIN M.R., *Performance of free space optical communication systems over exponentiated Weibull atmospheric turbulence channel for PPM and its derivatives*, Optik **127**(20), 2016: 9647–9657, DOI: [10.1016/j.ijleo.2016.07.036](https://doi.org/10.1016/j.ijleo.2016.07.036).
- [19] PRABU K., KUMAR D. S., SRINIVAS T., *Performance analysis of FSO links under strong atmospheric turbulence conditions using various modulation schemes*, Optik **125**(19), 2014: 5573–5581, DOI: [10.1016/j.ijleo.2014.07.028](https://doi.org/10.1016/j.ijleo.2014.07.028).
- [20] SINGH H., SAPPAL A.S., *Analytic and simulative comparison of turbulent FSO system with different modulation techniques*, Optics & Laser Technology **114**, 2019: 49–59, DOI: [10.1016/j.optlastec.2019.01.013](https://doi.org/10.1016/j.optlastec.2019.01.013).
- [21] BADAR N., JHA R.K., *Performance comparison of various modulation schemes over free space optical (FSO) link employing Gamma–Gamma fading model*, Optical and Quantum Electronics **49**(5), 2017: 192, DOI: [10.1007/s11082-017-1025-4](https://doi.org/10.1007/s11082-017-1025-4).
- [22] ISMAIL T., LEITGEB E., GHASSEMLOOY Z., AL-NAHHAL M., *Performance improvement of FSO system using multi-pulse pulse position modulation and SIMO under atmospheric turbulence conditions and with pointing errors*, IET Networks **7**(4), 2018: 165–172, DOI: [10.1049/iet-net.2017.0203](https://doi.org/10.1049/iet-net.2017.0203).
- [23] KHALLAFF H.S., SHALABY H.M.H., GARRIDO-BALSELLS J.M., SAMPEI S., *Performance analysis of a hybrid QAM-MPPM technique over turbulence-free and Gamma–Gamma free-space optical channels*, Journal of Optical Communications and Networking **9**(2), 2017: 161–171, DOI: [10.1364/jocn.9.000161](https://doi.org/10.1364/jocn.9.000161).
- [24] WANG P., YANG B., GUO L., SHANG T., *SER performance analysis of MPPM FSO system with three decision thresholds over exponentiated Weibull fading channels*, Optics Communications **354**, 2015: 1–8, DOI: [10.1016/j.optcom.2015.05.039](https://doi.org/10.1016/j.optcom.2015.05.039).
- [25] TODOROVIĆ J., SPALEVIĆ P., PANIĆ S., MILOSAVLJEVIĆ B., GLIGORIJEVIĆ M., *FSO system performance analysis based on novel Gamma–Chi-square irradiance PDF model*, Optica Applicata **51**(3), 2021: 335–348, DOI: [10.37190/oa210303](https://doi.org/10.37190/oa210303).
- [26] GRADSHTEYN I.S., RYZHIK I.M., *Table of Integrals, Series, and Products*, 7th ed., Elsevier Academic Press, USA, 2007.
- [27] BELMONTE A., KAHN J.M., *Performance of synchronous optical receivers using atmospheric compensation techniques*, Optics Express **16**(18), 2008: 14151–14162, DOI: [10.1364/oe.16.014151](https://doi.org/10.1364/oe.16.014151).
- [28] ESCRIBANO F. J., WAGEMAKERS A., *Performance analysis of QAM-MPPM in turbulence-free FSO channels: Accurate derivations and practical approximations*, IEEE Systems Journal **15**(2), 2021: 1753–1763, DOI: [10.1109/jsyst.2020.2986680](https://doi.org/10.1109/jsyst.2020.2986680).
- [29] BALAJI K.A., PRABU K., *Performance evaluation of FSO system using wavelength and time diversity over malaga turbulence channel with pointing errors*, Optics Communications **410**, 2018: 643–651, DOI: [10.1016/j.optcom.2017.11.006](https://doi.org/10.1016/j.optcom.2017.11.006).
- [30] The Wolfram Functions Site: Erfc functions. [Online] Available: <http://functions.wolfram.com/PDF/Erfc.pdf> (accessed March 2022).
- [31] The Wolfram Functions Site: MeijerG functions. [Online] Available: <http://functions.wolfram.com/PDF/MeijerG.pdf> (accessed March 2022).
- [32] PRUDNIKOV A.P., BRYCHKOV Y.A., MARICHEV O.I., *Integral and Series*, 2nd Ed., Fizmatlit, Moscow, Russia, 2003.
- [33] The Wolfram Functions Site: Erfc functions. [Online] Available: <http://functions.wolfram.com/PDF/Exp.pdf> (accessed March 2022).

*Received April 8, 2022
in revised form June 21, 2022*